Journal of Chemistry and Technologies, 2026, *34*(1), 86-97

Journal of Chemistry and Technologies

pISSN 2663-2934 (Print), ISSN 2663-2942 (Online).

journal homepage: http://chemistry.dnu.dp.ua
editorial e-mail: chem.dnu@gmail.com

UDC 546.224-31:547.435.1:547.281.1

ACID-BASE AND ELECTROCHEMICAL BEHAVIOR OF "SULFUR DIOXIDE – 1,3,5-TRIS-(2-HYDROXYETHYL)HEXAHYDROTRIAZINE – WATER" SOLUTIONS

Ruslan E. Khoma[1*], Anastasiya R. Kononchenko[1], Vira V. Veduta[1],
Serhiy V. Vodzinskii[1], Kostiantyn I. Semenov[1], Vasyl S. Kovtun[1], Dmitro V. Shoshin[2]
[1]*Odesa I. I. Mechnikov National University, 2 Vsevoloda Zmienko str., Odesa, 65082, Ukraine*
[2]*National Technical University «Dnipro Polytehnic», Dmytro Yavornitsky av., 19, Dnipro, 49005*
Received 28 August 2025; accepted 11 November 2025; available online 23 March 2026

Abstract

Establishing the features of acid-base and electrochemical behavior in "sulfur dioxide – 1,3,5-tris-(2-hydroxyethyl)hexahydrotriazine – water" solutions is undoubtedly an actual and important task. A pH-, redox-, and conductometric studies of protolytic equilibria were carried out for the solutions containing 1,3,5-tris-(2-hydroxyethyl)hexahydrotriazine (TZ; the reaction product of monoethanolamine with formaldehyde interaction), its protonated form (TZH^+), N-(2-hydroxyethyl)aminomethanesulfonic acid (HEAMSA), and its anion, N-(2-hydroxyethyl)aminomethane-sulfonate (HEAMS) at a constant total content of amine nitrogen 0.1 mol/L with varying content of absorbed sulfur dioxide $0 \le Q_{SO_2} \le 0.12$ mol/L at temperature range 273–313 K. It was shown that the addition of formaldehyde to solutions of "sulfur dioxide – monoethanolamine – water" leads to a decrease in their pH by 0.09–4.75 units, which is obviuosly caused by the formation of HEAMSA. The symbiotic nature of the change in ΔpH values with temperature (SO_2 : N < 1.0 : 2.0) is noted at the same content of components in the solutions. Conductometry data indicate the association of free monoethanolamine, its ammonium sulfites and hydrosulfites into less mobile TZ, TZH^+, HEAMSA and $HEAMS^-$. Based on the developed mathematical model using pH-metry data, the ion-molecular component composition of "sulfur dioxide – 1,3,5-tris-(2-hydroxyethyl)hexahydrotriazine – water" solutions at 273–313 K was calculated. The concentration dependences on the ionic strength of the solutions were obtained. The concentration constants of TZ protonation and HEAMSA dissociation were estimated. It was shown that under the experimental conditions the thermodynamic dissociation constant of HEAMSA is practically independent on temperature and is equal to 10.14 ± 0.08. The obtained results are recommended to be used in the development of effective chemisorbents of sulfur dioxide.

Key words: sulfur dioxide; monoethanolamine; formaldehyde; 1,3,5-tris-(2-hydroxyethyl)hexahydrotriazine; acid-base interaction; specific electrical conductivity.

КИСЛОТНО-ОСНОВНА ТА ЕЛЕКТРОХІМІЧНА ПОВЕДІНКА РОЗЧИНІВ ДІОКСИД СІРКИ – 1,3,5-ТРИ-(ГІДРОКСИЕТИЛ)ГЕКСАГІДРОТРИАЗИН – ВОДА

Руслан Є. Хома[*1], Анастасія Р. Кононченко[1], Віра В. Ведута[1],
Сергій В. Водзінський[1], Костянтин І. Семенов[1], Василь С. Ковтун[1], Дмитро В. Шошин[2]
[1]*Одеський національний університет імені І. І. Мечникова,вул. Змієнка Всеволода, 2, Одеса, 65082*
[2]*Національний технічний університет «Дніпровська політехніка», пр-т Дмитра Яворницького, 19, Дніпро, 49005*

Анотація

Встановлення особливостей кислотно-основної та електрохімічної поведінки в розчинах «діоксид сірки – 1,3,5-трис-(2-гідроксиетил)гексагідротриазин – вода» є безумовно актуальним завданням. Здійснені pH-, редокс- та кондуктометричне вивчення протеолітичних рівноваг у досліджуваних розчинах за сумарного вмісту амінного азоту в складі 1,3,5-тріс-(2-гідроксиетил)гексагідротриазину (TZ; продукту взаємодії моноетаноламіну із формальдегідом), його протонованої форми (TZH^+), N-(2-гідроксиетил)амінометан-сульфокислоти (HEAMSA) та N-(2-гідроксиетил)амінометан-сульфонат іону ($HEAMS^-$) 0.1 моль/л та за вмісту поглинутого діоксиду сірки $0 \le Q_{SO_2} \le 0.12$ моль/л в області температур 273–313 К. Додавання формальдегіду до розчинів «діоксид сірки – моноетаноламін – вода» призодить до пониження їх pH на 0.09 ÷ 4.75 од., що очевидно спричинено утворенням HEAMSA. Відмічено симбатний характер зміни величин ΔpH з температурою за однакового вмісту компонентів у розчинах (SO_2 : N < 1.0 : 2.0). Дані кондуктометрії вказують на зв'язування вільного моноетаноламіну, його амонієвих сульфітів та гідросульфітів у менш рухливі TZ, TZH^+, HEAMSA та $HEAMS^-$. На основі розробленої математичної моделі з використанням даних pH-метрії розрахований йон-молекулярний компонентний склад розчинів «діоксид сірки – 1,3,5-трис-(2-гідроксиетил) гексагідротриазин – вода» за 273–313 К. Отримані концентраційні залежності іонної сили розчинів. Оцінені концентраційні константи протонування TZ та дисоціації HEAMSA. Показано, що в умовах експерименту термодинамічна константа дисоціації HEAMSA майже не залежить від температури і дорівнює 10.14 ± 0.08. Отримані результати рекомендується використовувати під час розробки ефективних хемосорбентів SO_2.

**Corresponding author: e-mail: rek@onu.edu.ua*

Journal of Chemistry and Technologies, 2026, *34*(1), 86-97

Ключові слова: діоксид сірки; моноетаноламін; формальдегід; 1,3,5-трис-(2-гідроксиетил)гексагідротриазин; кислотно-основна взаємодія; питома електропровідність.

Introduction

Scientific interest in N-derivatives of aminomethanesulfonic acid (YAMSA), particularly N-(2-hydroxyethyl)aminomethanesulfonic acid (HEAMSA), origins from their specific physicochemical properties and a wide range of pharmaceutical activities [1–14]. They are low-toxic compounds having antimicrobial and antiviral properties, synergistically enhancing the antioxidant activity of quercetin [1; 3–5], potential components of electrolytes in vanadium redox flow batteries [13]. YAMSA are also used as components of Good's buffer solutions in biological and biochemical studies [1; 2; 4; 6; 10], calcium scale inhibitors [9], catalysts for effective cellulose hydrolysis into glucose [14], etc. A detailed overview of the applications of these compounds is given in [1]. One of the methods for synthesizing HEAMSA is the saturation of aqueous solutions of 1,3,5-tris-(2-hydroxyethyl)hexa-hydrotriazine, commonly called triazine (TZ), with gaseous sulfur dioxide [4]. To date, no researches aimed at studying the mechanism of the indicated reaction have been found in the literature, apart from the works of our research group.

TZ is synthesized by reacting of monoethanolamine (MEA) with formaldehyde at a molar ratio of 1.0 : 1.0 [15; 16]. It is a biocide used in lubricating and cooling fluids and paints [17; 18], as well as an active component of liquid H_2S and alkyl mercaptan chemisorbents [19–23]. 1,3,5-Triazines are used to obtain various forms (polymeric, supported, etc.) of effective SO_2 chemisorbents [4; 24; 25].

However, there are no literature data on the changes in acid-base and electrochemical characteristics during the absorption of sulfur dioxide by aqueous TZ solutions. These properties depend on the ionic-molecular composition of the solutions, the constants of the dissociation processes occurring within them [4]. Therefore, the identification of the features of acid-base and electrochemical behavior during the SO_2 interaction with aqueos TZ solutions is, undoubtedly, a relevant task. In this work, the methods of pH-, redox- and conductometric titration were used to investigate the interaction of an aqueous solution of TZ with gaseous SO_2. These methods were successfully used for establishing the ionic-molecular composition of solutions "sulfur dioxide – N-containing organic base – water" and calculating the formation constants of ammonium sulfites, hydrosulfites and pyrosulfites, as well as anion-molecular and intermolecular (charge transfer) complexes [4; 26; 27].

Experimental part

Reagents monoethanolamine (MEA, "PA" qualification) and paraform ("for synthesis"), as well as gaseous SO_2 from a gas cylinder were used without additional purification. As a chemisorbent in this work, an aqueous solution of TZ was used. It was obtained by the addition of equimolar amount of paraform to an aqueous 0.1 mol/L solution of MEA at room temperature [15].

The potentiometric measurements were performed using an EV-74 universal ionometer and a pH-150M pH meter. The accuracy of the redox potential measurement for the EV-74 was ± 1 mV. The accuracy of the pH measurement for the pH-150M was ± 0.02. Conductometric studies were performed on a SensION5 conductometer using the electrode for electrical conductivity measuring Sension HACH 5197500.

For potentiometric titration of aqueous solutions with sulfur dioxide a laboratory setup [26] is used. The main element of the setup is a cylindrical thermostated measuring cell, with the top equipped with electrodes, a temperature sensor and a device for bubbling SO_2. In the measuring cell, along with pneumatic mixing, mechanical mixing is used, which ensures almost perfect mixing of the reagents.

Gaseous sulfur dioxide is continuously bubbled at a constant volume rate through a thermostated cell containing 250 ml of model solution. The volumetric flow rate of sulfur dioxide is 8.0 ml/min. Under these conditions, a bubbling mode is ensured, in which the mass transfer coefficient between the gas and liquid phases is sufficiently high. This achieves almost complete interaction between the gas and the absorbent.

Amount of SO_2, that has reacted with the components of the sorption system is calculated by the formula (1):

$$Q = \frac{q \cdot (C^S_{SO_2} - C^F_{SO_2})}{V_s}, \qquad (1)$$

whereas Q is amount of SO_2, (mol/L); V_s is solution volume, (ml); $C^S_{SO_2}$ and $C^F_{SO_2}$ are concentrations of SO_2 in the gas phase before and after the reaction, (mol/L); q is the volume of gas (ml) passed through the cell during the

experiment time τ. Provided that $C^S_{SO_2} >> C^F_{SO_2}$, Q, in the first approximation can be calculated by the formula (2):

$$Q = \frac{\tau \cdot v_g}{V_p \cdot V_m}, \quad (2)$$

whereas τ is time of SO_2 passage through the chemisorption system, min; v_g is SO_2 volume velocity, mL/min; V_p – volume of chemisorption solution, L; V_m is molar volume, L/mol (under normal conditions $V_m(SO_2)$ = 21,89 L/mol).

Results and discussion

pH-metry of "SO_2 – TZ – H_2O" solutions

Fig. 1a shows the data of pH-metric titration of an aqueous solution of TZ with gaseous sulfur dioxide at temperature range 273÷313 K. All pH = f(Q_{SO_2}) curves have two jumps, which correspond to the maxima on the differential curves (Fig. 1b), except for 308 K. The first effects on the integral curves occur at the stoichiometric ratio SO_2 : N = 1.0 : 15.0 (at 293, 308 and 313 K) and 1.0 : 10.0 (at 273, 283 and 300 K); the second ones occur at SO_2 : N = 2.0 : 3.0 at all studied temperatures. In addition to the above, at 273 K, a maximum is observed on the integral curve at SO_2 : N = 1.0 : 5.0 (Fig. 1a, curve 1), which corresponds to a discontinuity of the second kind on the differential curve (Fig. 1b, curve 1). On the differential curve at 283 K (Fig. 1b, curve 2) an additional minimum is observed at the same stoichiometric ratio (1.0 : 5.0).

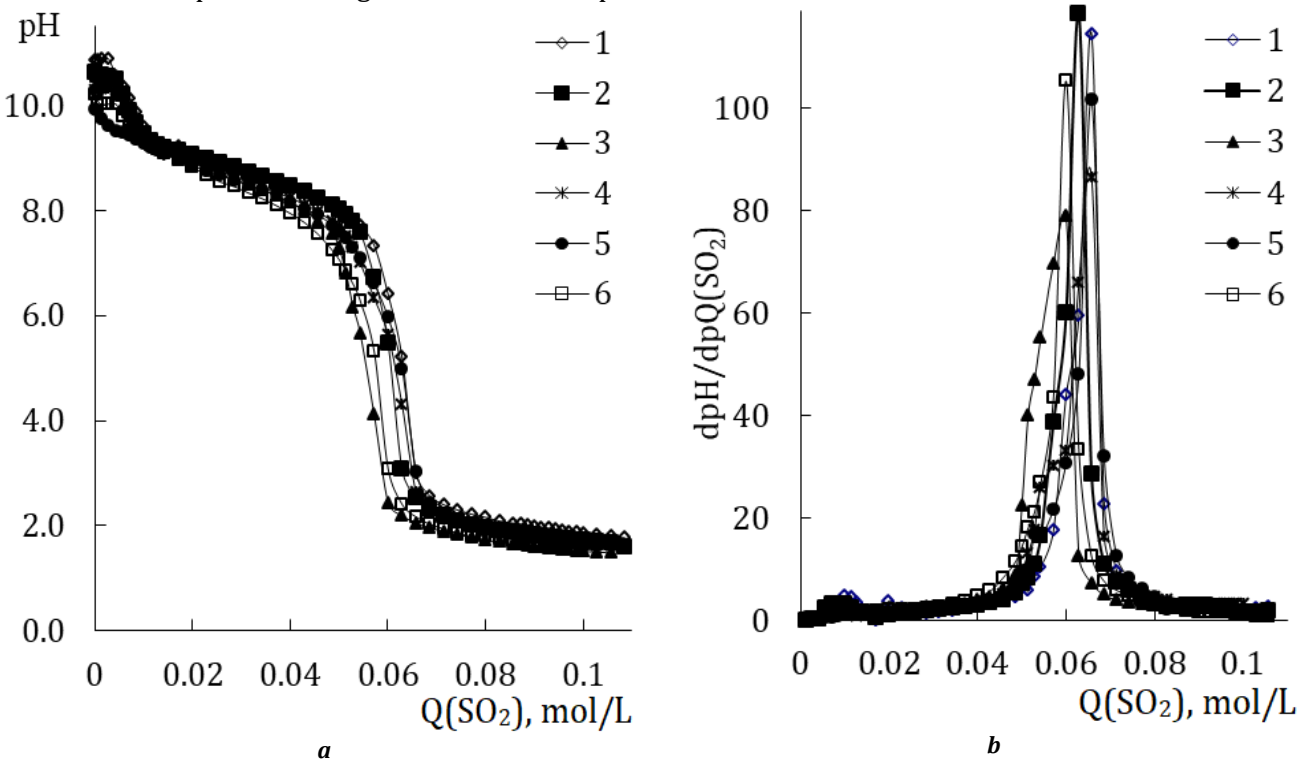

a *b*

Fig. 1. Integral (a) and differential (b) pH-metric titration curves of aqueous 0.1 mol/L TZ solution with gaseous SO_2

To identify the nature of the influence of formaldehyde addition on the interaction in "SO_2 – MEA – H_2O" solutions, comparative pH-metry was carried out (Fig. 2) taking into account previously published experimental data [4]. The introduction of CH_2O into the above aqueous solutions leads to a decrease in their pH by 0.09 ÷ 4.75 units. An increase in the SO_2 content in TZ-based absorption solutions causes a decrease in ΔpH, passing through local minima corresponding to the first maxima on the differential curves (Fig. 1*b*; Table 1). Further addition of sulfur dioxide leads to a gradual increase in the values ΔpH, reaching maximum values at SO_2 : N ≈ 1.0 : 2.0 in a weakly alkaline environment (pH 7.33 ÷ 7.78) at 273 ÷ 300 K. Further on, there is a sharp decrease in ΔpH passing through a global minima corresponding to local maxima on the differential curves.

Negative values of ΔpH could be explained by the fact that the addition of formaldehyde to "SO_2 – MEA – H_2O" solutions causes the formation of HEAMSA [4], which is actually a stronger acid in the first degree of dissociation than SO_2 hydrate (the so-called "sulfurous acid") [4; 6]. There is a symbiotic nature of the change in the values of

Journal of Chemistry and Technologies, 2026, *34*(1), 86-97

ΔpH with temperature at the same content of components in solutions (SO_2 : N < 1.0 : 2.0), which is described by equation (3), the parameters of eq.3 are given in Table 2. This indicates a decrease in the differentiating effect of formaldehyde on the pH of "SO_2 – MEA – H_2O" solutions with increasing temperature.

$$\Delta pH = A_i + B_i \cdot T \quad (3)$$

In this case, the parameters A_i and B_i (Table 2) are related by a linear relationship (4).

$$B_i = -0.003151 \cdot A_i \cdot T;\ R^2 = 0.9990 \quad (4)$$

Taking into account above equations (3) and (4), we have an equation (5).

$$\Delta pH = A_i - 0.003151 \cdot A_i \cdot T;\ R^2 = 0.9990 \quad (5)$$

Table 1

Characteristics of pH-metric titration curves of aqueous 0.1 mol/L TZ solution with gaseous SO_2

Effect	Q_{SO_2}/Q_N	Integral curve		Differential curve		Difference curve	
		Shape	pH	Shape	dpH/dpQ_{SO_2}	Shape	ΔpH
				273 K			
I	1.0 : 10.0	jump	9.57	maximum	4.63	minimum	-2.94
II	1.0 : 5.0	maximum	8.97	second kind discontinuity	–	minimum	-2.59
III	2.0 : 7.0	–	8.70	minimum	1.31	–	-2.43
IV	4.0 : 7.0	–	7.33	–	17.5	maximum	-0.71
V	2.0 : 3.0	jump	2.99	maximum	115	minimum	-4.67
				283 K			
I	1.0 : 10.0	jump	9.45	maximum	3.20	minimum	-2.12
II	1.0 : 5.0	–	9.06	minimum	0.50	plateau	-1.90
III	1.0 : 2.0	–	7.78	–	10.9	maximum	-0.34
IV	2.0 : 3.0	jump	3.07	maximum	118	minimum	-4.57
				293 K			
I	1.0 : 15.0	jump	9.93	maximum	3.09	minimum	-1.68
II	1.0 : 2.0	–	7.56	–	8.73	maximum	-0.79
III	2.0 : 3.0	jump	2.44	maximum	78.8	minimum	-4.74
				300 K			
I	1.0 : 10.0	jump	9.47	maximum	2.69	minimum	-0.96
II	1.0 : 5.0	–	8.95	–	1.79	minimum	-0.88
III	1.0 : 2.0	–	7.51	–	13.1	maximum	-1.03
IV	2.0 : 3.0	jump	2.63	maximum	86.5	minimum	-4.13
				308 K			
I	1.0 : 15.0	jump	9.70	–	1.83		
II	2.0 : 3.0	jump	3.03	maximum	102		
				313 K			
I	1.0 : 15.0	jump	9.62	–	1.75	–	-0.28
II	2.0 : 3.0	jump	3.08	maximum	105	minimum	-4.08

Concentration dependences $A_i = f(Q_{SO_2})$ are described by the equations (4) and (5).

$$A_i = 7.97 + 1847.4 \cdot Q_{SO_2} - 67874(Q_{SO_2})^2 \quad (4)$$

($Q_{SO_2} \le 0.02$ M); $R^2 = 0.9278$; n = 11

$$A_i = 17.11 + 138.8 \cdot Q_{SO_2} - 4222.8(Q_{SO_2})^2$$

($0.02 \le Q_{SO_2} \le 0.0486$ mol/L); (5)

$R^2 = 0.9704$; n = 11

Redoxmetry of "SO_2 – TZ – H_2O" solutions

The results of the redoxmetric study of the interaction in the "SO_2 – TZ – H_2O" solutions are shown in Fig. 3, 4. When the amount of absorbed sulfur dioxide by the studied TZ solution increases to 0.06 mol/L, the redox potential values increase in the entire range of studied temperatures (Fig. 3a), except for 300 K (curve 5), in contrast to published results for ethanolamines solutions [4].

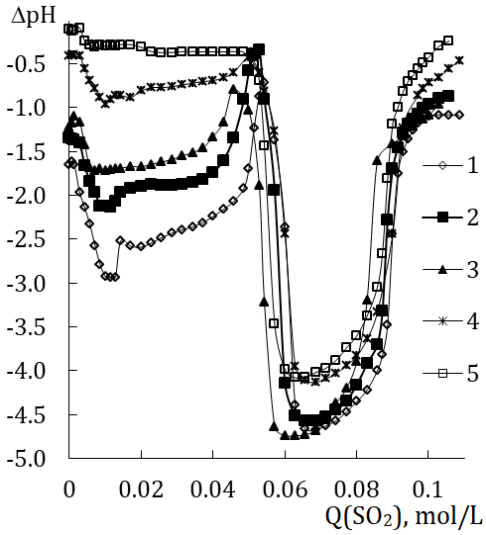

Fig. 2. Comparative pH-metry of "SO_2 – TZ – H_2O" (*a*) and "SO_2 – $NH_2CH_2CH_2OH$ – H_2O" (*b*) [4] solutions. ΔpH = pH_a – pH_b. T (K): 273 – 1; 283 – 2; 293 – 3; 300 – 4; 313 – 5

Journal of Chemistry and Technologies, 2026, *34*(1), 86-97

Table 2

Equation (3) parameters. n = 5

Q_{SO_2}, mol/L	$-A_i$	B_i	R^2
0.00286	12.941	0.0411	0.9441
0.00429	15.055	0.0481	0.9580
0.00572	15.734	0.0497	0.9451
0.00715	16.951	0.0533	0.9309
0.00858	18.427	0.0580	0.9556
0.01001	20.193	0.0637	0.9813
0.01144	20.764	0.0655	0.9856
0.01287	21.109	0.0667	0.9825
0.01430	20.885	0.0661	0.9769
0.01716	18.130	0.0570	0.9682
0.02002	18.334	0.0577	0.9733
0.02288	18.301	0.0576	0.9637
0.02574	17.705	0.0556	0.9578
0.02860	17.303	0.0543	0.9599
0.03146	17.015	0.0534	0.9612
0.03432	16.813	0.0528	0.9623
0.03718	16.604	0.0521	0.9634
0.04004	16.231	0.0510	0.9641
0.04290	15.569	0.0489	0.9734
0.04576	14.702	0.0462	0.9743
0.04862	13.501	0.0426	0.9180

On the integral redoxmetric titration curves there are two jumps at 273 and 283 K (Fig. 3a; Table 3) at the same SO_2 : N ratios same to the jumps on the integral pH-metric curves (Fig. 1a; Table 1). At other temperatures (293 ÷ 313 K) only one jump on the integral redoxmetric curves is observed. In addition to the above, the curves under discussion additionally contain inflections, plateaus, discontinuities of the second kind, as well as extrema (minima and maxima). These effects correspond to extrema and breaks on the corresponding differential redoxmetric curves (Fig. 3b; Table 3), as well as to mostly the same effects on the difference curves (Fig. 4; Table 3).

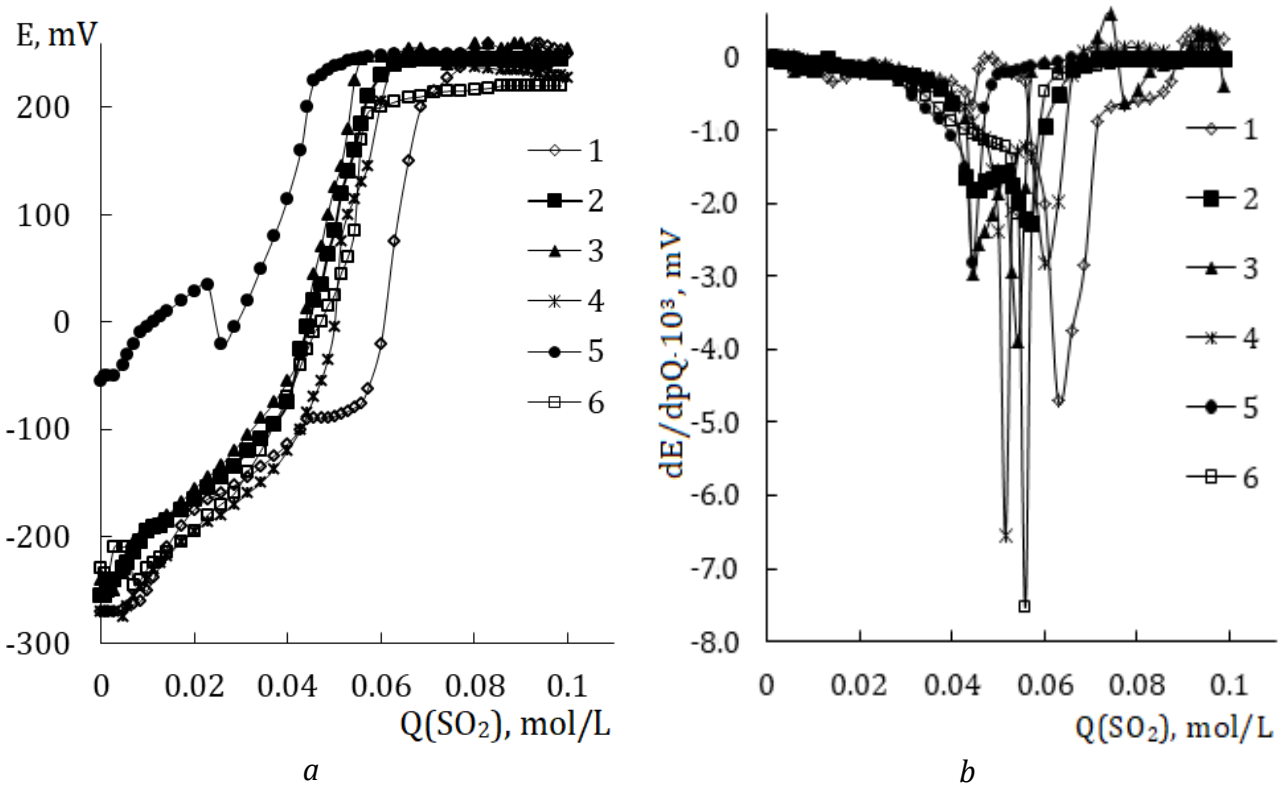

a *b*

Fig. 3. Integral (a) and differential (b) redoxmetric titration curves of aqueous 0.1 mol/L TZ solution with gaseous SO_2

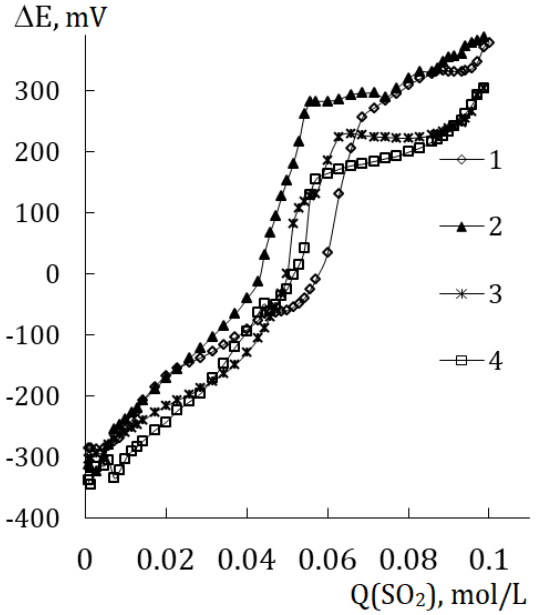

Fig. 4. Comparative redoxmetry of "SO_2 – TZ – H_2O" (*a*) and "SO_2 – $NH_2CH_2CH_2OH$ – H_2O" (*b*) [4] solutions. ΔE = E_a – E_b
T (K): 273 – 1; 293 – 2; 300 – 3; 313 – 4

Table 3

Characteristics of redoxmetric titration curves of aqueous 0.1 mol/L TZ solution with gaseous SO_2

Effect	Q_{SO_2}/Q_N	Integral curve		Differential curve		Difference curve	
		Shape	E, mV	Shape	dE/dpQ_{SO_2}, mV	Shape	ΔE, mV
				273 K			
I	1.0 : 8.0	jump	-195	maximum	–340	jump	–210
II	1.0 : 4.0	inflection	-90	minimum	–100	–	–145
III	0.46	plateau	-85	maximum	–660	plateau	–65
IV	1.0 : 2.0	inflection	150	minimum	0	inflection	–60
V	2.0 : 3.0	jump	150	minimum	–4700	jump	130
				283 K			
I	1.0 : 10.0	inflection	-190	maximum	–149		
II	1.0 : 8.0	inflection	20	minimum	–20		
III	1.0 : 2.0	jump	245	minimum	–1813		
V	2.0 : 3.0	jump	245	minimum	–2274		
				293 K			
I	1.0 : 10.0	inflection	125	minimum	–175	inflection	–255
II	1.0 : 2.0	jump	250	minimum	–2950	jump	155
III	3.0 : 5.0	plateau	240	minimum	–3890	plateau	280
IV	3.0 : 4.0	minimum	240	minimum	–128	inflection	290
				300 K			
I	1.0 : 2.0	jump	250	minimum	–6540	jump	0
II	2.0 : 3.0	maximum	250	minimum	–2832	plateau	229
				308 K			
I	1.0 : 4.0	second kind discontinuity	225	inflection	–143		
II	1.0 : 2.0	jump	225	minimum	–2808		
				313 K			
I	1.0 : 10.0	minimum	245	inflection	–63	minimum	–335
II	1.0 : 2.0	jump	25	inflection	–1087	jump	0
III	3.0 : 5.0	plateau	200	minimum	–7534	plateau	165

Conductometry of "SO_2 – TZ – H_2O" solutions

Data on the conductometric study of the electrochemical properties of "SO_2 – TZ – H_2O" solutions are shown in Fig. 5.

Journal of Chemistry and Technologies, 2026, *34*(1), 86-97

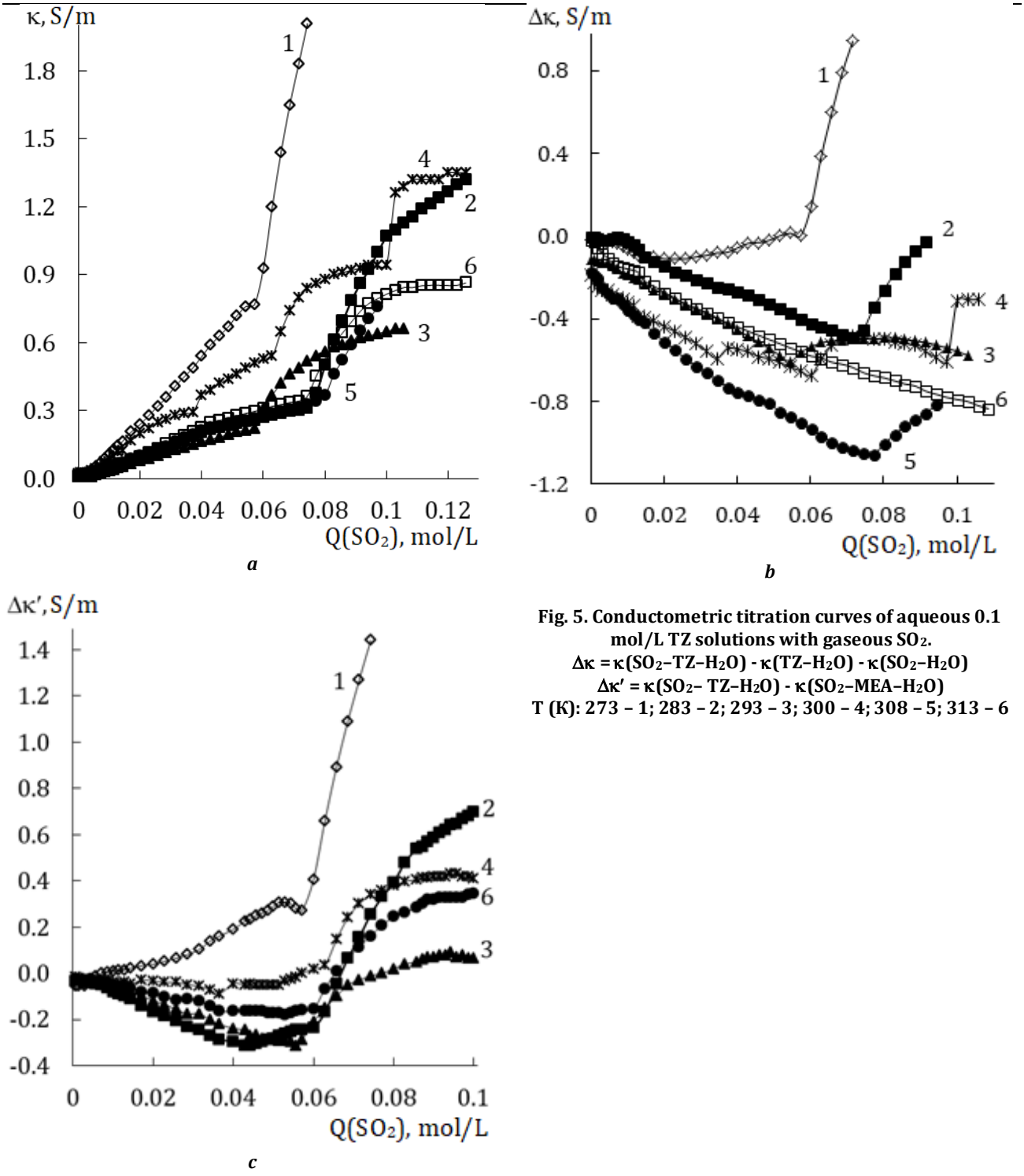

a ***b*** ***c***

Fig. 5. Conductometric titration curves of aqueous 0.1 mol/L TZ solutions with gaseous SO_2.
$\Delta\kappa = \kappa(SO_2–TZ–H_2O) - \kappa(TZ–H_2O) - \kappa(SO_2–H_2O)$
$\Delta\kappa' = \kappa(SO_2– TZ–H_2O) - \kappa(SO_2–MEA–H_2O)$
T (K): 273 – 1; 283 – 2; 293 – 3; 300 – 4; 308 – 5; 313 – 6

On the curves of $\kappa = f(Q_{SO_2})$ functions at temperatures of 273 and 293 K (Fig. 5*a*, curves 1 and 3; Table 4) only one inflection is observed, whereas at the other temperatures (Fig. 5*a*, curves 2, 4, 5; Table 4) there are two inflections. At temperature range 283÷313 K throughout all the studied amounts of Q_{SO_2} at 273 K and ratio (SO_2 : N $\leq$ 1,0 : 2,0) $\Delta\kappa$ (Fig. 5*b*) acquires negative values, which are associated with the formation of weakly dissociated compounds in the studied solutions. On the curves of $\Delta\kappa = f(Q_{SO_2})$ (Fig. 4*b*) in the temperature range 283÷300 K new effects (breaks, maxima and minima) appear, which are not observed on the $\kappa = f(Q_{SO_2})$ dependencies.

Journal of Chemistry and Technologies, 2026, *34*(1), 86-97

Table 4

Characteristics of conductometric titration curves of aqueous 0.1 mol/L TZ solution with gaseous SO_2

Effect	Q_{SO_2}/Q_N	$\kappa = f(Q_{SO_2})$		$\Delta\kappa = f(Q_{SO_2})$		$\Delta\kappa' = f(Q_{SO_2})$	
		Shape	κ, S/m	Shape	Δκ, S/m	Shape	Δκ′, S/m
				273 K			
I	1.0 : 4.0	–	0.30	minimum	−0.11	inflection	0.07
II	5.0 : 11.0	–	0.63	inflection	−0.03	–	0.25
III	1.0 : 2.0	–	0.70	inflection	−0.01	maximum	0.29
IV	3.0 : 5.0	inflection	0.77	inflection	0	minimum	0.27
				283 K			
I	1.0 : 10.0	–	0.038	maximum	0	inflection	−0.079
II	2.0 : 5.0	inflection	0.203	–	−0.255	minimum	−0.313
III	1.0 : 2.0	–	0.239	inflection	−0.312	–	−0.271
IV	3.0 : 5.0	–	0.269	–	−0.399	inflection	−0.235
V	6.0 : 8.0	inflection	0.310	minimum	−0.488	inflection	0.256
VI	6.0 : 7.0	–	0.695	–	−0.180	inflection	0.539
				293 K			
I	1.0 : 5.0	–	0.100	inflection	−0.259	inflection	−0.049
II	1.0 : 3.0	–	0.131	–	−0.360	inflection	−0.174
III	4.0 : 7.0	inflection	0.222	minimum	−0.607	minimum	−0.314
IV	2.0 : 3.0	–	0.370	–	−0.516	inflection	−0.050
V	6.0 : 7.0	–	0.590	maximum	−0.493	–	0.050
				300 K			
I	1.0 : 3.0	–	0.282	minimum	−0.557	minimum	−0.009
II	2.0 : 5.0	inflection	0.370	–	−0.542	inflection	−0.005
III	3.0 : 5.0	inflection	0.530	–	−0.652	inflection	0
IV	2.0 : 3.0	–	0.540	minimum	−0.673	inflection	0.035
V	6.0 : 8.0	–	0.840	maximum	−0.483	inflection	0.340
				313 K			
I	1.0 : 4.0	–	0.135	–	−0.300	inflection	−0.115
II	2.0 : 5.0	inflection	0.226	–	−0.420	inflection	−0.163
III	3.0 : 5.0	–	0.309	–	−0.560	inflection	−0.155
IV	6.0 : 8.0	inflection	0.365	inflection	−0.635	–	0.162
V	6.0 : 7.0	–	0.644	–	−0.700	inflection	0.319

Negative values of Δκ′, characterizing the effect of formaldehyde addition on the electrochemical properties of "SO_2 – $NH_2CH_2CH_2OH$ – H_2O" solutions at $SO_2 : N \leq 2/0 : 3/0$ and 283 ÷ 313 K (Fig. 5*c*), indicate the binding of free monoethanolamine, its ammonium sulfites and hydrosulfites to TZ, protonated TZ (**TZH**$^+$), HEAMSA and N-(2-hydroxyethyl)amino-methanesulfonate (**HEAMS**$^-$). The last three are characterized by lower mobility than the ionic components of the system "SO_2 – $NH_2CH_2CH_2OH$ – H_2O". Positive values of Δκ′ are obviously caused by the dissociation of HEAMSA.

Composition of "SO_2 – TZ – H_2O" solutions

Based on the above potentiometric and conductometric studies, as well as known literature data [1; 4-8; 26-29] it can be stated that the following processes (8) – (16) are realized in the studied *"SO_2 – TZ – H_2O"* solutions.

$$3mYNH_2 + 3(CH_2O)_m \xrightarrow{H_2O} \text{m}\ \text{(TZ)} + 3mH_2O \qquad (8)$$

Y = CH_2CH_2OH

$$\text{TZ} + H_2O \underset{}{\overset{K_b}{\rightleftharpoons}} \text{TZH}^+ + OH^- \qquad (9)$$

Journal of Chemistry and Technologies, 2026, *34*(1), 86-97

$$SO_2^g \rightleftarrows SO_2^s \quad (10)$$

$$SO_2^s + H_2O \rightleftarrows SO_2{\cdot}H_2O \quad (11)$$

$$SO_2{\cdot}H_2O \overset{K_1}{\rightleftarrows} H^+ + HSO_3^- \quad (12)$$

$$2\,HSO_3^- \overset{K^*}{\rightleftarrows} S_2O_5^{2-} + H_2O \quad (13)$$

$$HSO_3^- \overset{K2}{\rightleftarrows} H^+ + SO_3^{2-} \quad (14)$$

where SO_2^g and SO_2^s is sulfur dioxide in the gas phase and dissolved in water respectively [4].

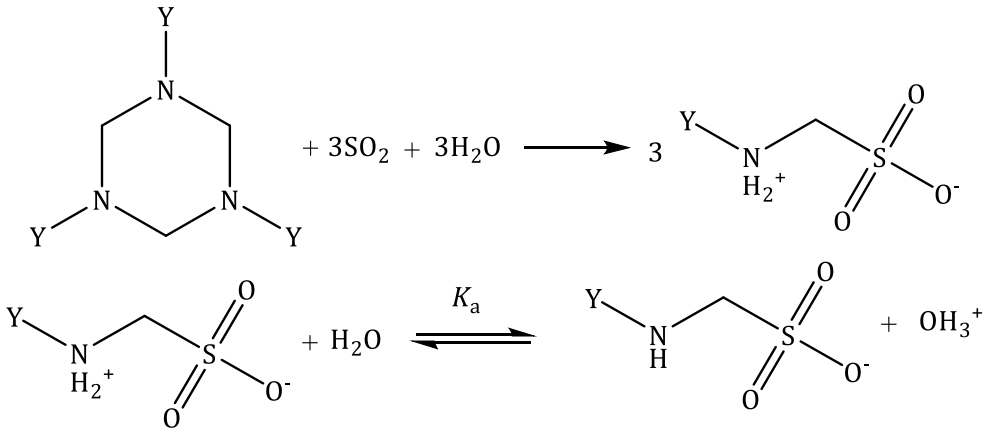

(15)

(16)

The material balance for S and N is described by equations (17) and (18), respectively. The condition of electroneutrality has the form (19).

$$Q_S = [SO_2{\cdot}H_2O] + [HSO_3^-] + 2[S_2O_5^{2-}] + \\ +[SO_3^{2-}] + [HEAMSA] + [HEAMS^-] \quad (17)$$

$$Q_N = 3{\cdot}[TZ] + 3{\cdot}[TZH^+] + [HEAMSA] + \\ +[HEAMS^-] \quad (18)$$

$$[HSO_3^-] + 2[S_2O_5^{2-}] + 2[SO_3^{2-}] + \\ + [HEAMS^-] + [OH^-] = [H_3O^+] + [TZH^+] \quad (19)$$

The solution of the system of mathematical equations (17–19) using the pH-metric titration data (Fig. 1a) allowed us to establish the component (ionic and molecular) composition of the chemical system "SO_2–TZ–H_2O" (for example, Fig. 6), analogously to [4].

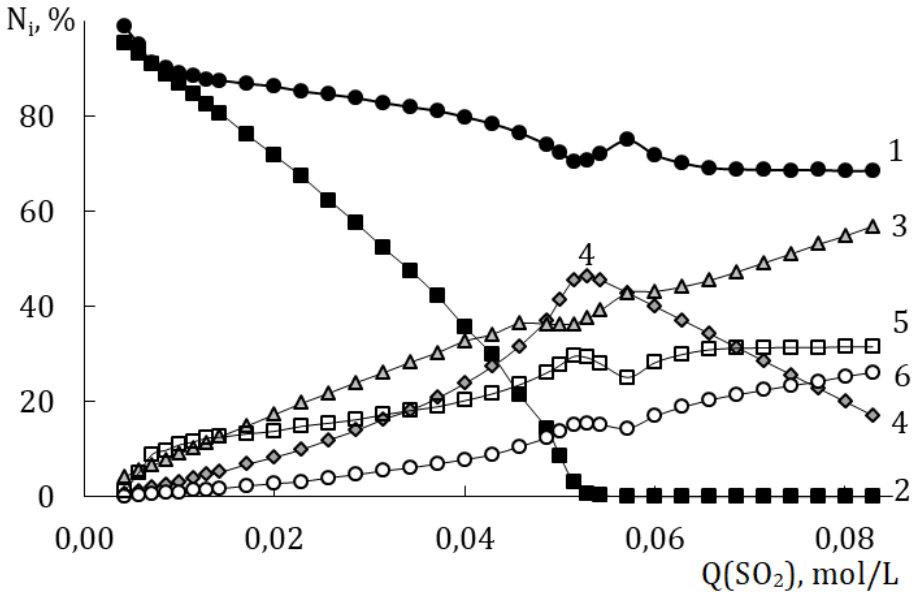

Fig. 6. Ratio of various forms of components in "SO_2 – TZ – H_2O" solutions as a function of Q_{SO_2} at 293 K. N_i – mole fraction N_1 = [HEAMSA]/Q_S, N_2 = 3[TZ]/Q_N, N_3 = [HEAMSA]/Q_N, N_4 = 3[TZH^+]/Q_N, N_5 = [$HEAMS^-$]/Q_S, N_6 = [$HEAMS^-$]/Q_N.

Journal of Chemistry and Technologies, 2026, *34*(1), 86-97

According to Fig. 6, an increase in the amount of absorbed SO_2 (from $4.3 \cdot 10^{-3}$ to $5.0 \cdot 10^{-2}$ mol/L) causes an increase in the molar fractions of HEAMSA (curve 3) and $HEAMS^-$ (curve 6) relative to the total nitrogen content. It is observed due to the acid-catalyzed hydrolytic decomposition of TZ (curve 2; equation 13). In this case, protonation of TZ occurs (reaction 7) with the formation of TZH^+ (curve 4). The accumulation of H_3O^+ ions (Fig. 1, curve 4) occurs due to dissociation of the zwitterionic form HEAMSA (Fig. 6, curve 1; reaction 14) with the formation of the anionic form $HEAMS^-$ (curves 5 and 6). Further introduction of SO_2 (from $5.0 \cdot 10^{-2}$ to $8.3 \cdot 10^{-2}$ M) leads to the transformation of the protonated form TZH^+ (curve 4) into HEAMSA (curve 3) and $HEAMS^-$ (curves 5 and 6).

In this case, the maxima on the curves $TZH^+/Q_N = f(Q_{SO_2})$, $[HEAMS^-]/Q_S = f(Q_{SO_2})$ and $[HEAMS^-]/Q_N = f(Q_{SO_2})$ (curves 4-6, respectively) and minima on the curves $[HEAMSA]/Q_S = f(Q_{SO_2})$ and $[HEAMSA]/Q_N = f(Q_{SO_2})$ (curves 1 and 3, respectively) correspond to the stoichiometric ratio $SO_2 : TZ = 1.0 : 2.0$, which is reflected in the pH-, redox- and conductometric data (Fig. 1–4; Tables 1–3). The minima on the curves $[HEAMS^-]/Q_S = f(Q_{SO_2})$ and $[HEAMS^-]/Q_N = f(Q_{SO_2})$ (curves 5 and 6, respectively) and the maximum on the curve $[HEAMSA]/Q_S = f(Q_{SO_2})$ (curve 1) correspond to $SO_2 : TZ = 4.0 : 7.0$, which is accompanied by corresponding effects on the conductometric curves (Fig. 4; Table 4).

The ionic strength (μ, M) of the solutions was calculated by the following formula (20).

$$\mu = ½([H_3O^+] + [OH^-] + [TZH^+] + [HSO_3^-] + 4\cdot[S_2O_5^{2-}] + 4\cdot[SO_3^{2-}] + [HEAMS^-] + 4\cdot[HEAMSA]) \quad (20)$$

In this case concentration dependence $\mu = f(Q_{SO_2})$ in the range $0.02 \le Q_{SO_2} \le 0.05$ mol/L is described by equation (21), the parameters of which are given below in Table 5.

$$\mu = A_i + B_i \cdot Q_{SO_2} + C_i \cdot (Q_{SO_2})^2 \quad (21)$$

Also, the parameters of equation (21) are interconnected by linear dependencies (22) and (23).

$$B_i = 0.0970 - 96.04 \cdot A_i; \quad R^2 = 0.9879;\ n = 6 \quad (22)$$

$$C_i = 0.8869 + 1321.5 \cdot A_i; \quad R^2 = 0.9507;\ n = 6 \quad (23)$$

Using the obtained data, the pK_b values of TZ (equation 7) and pK_a values of HEAMSA (equation 14; Table 5) were calculated. The temperature dependence of pK_b(TZ) on the temperature in the range of 273 ÷ 300 K is described by equation (24).

$$pK_b = -4.00 + 2958.8/T; \quad R^2 = 0.9523;\ n = 4 \quad (24)$$

It should be noted that under the experimental conditions of [23] pK_b(TZ) is equal to 6.43 at 298 K.

The concentration dependences of pK_a(HEAMSA) on the ionic strength in the range of $0.02 \le Q_{SO_2} \le 0.05$ mol/L are described by equation (25), corresponding parameters are given in Table 5.

$$pK_a(\text{HEAMSA}) = A_i + B_i \cdot \mu \quad (25)$$

According to the calculated results, the values of A_i constants in equation (25) practically do not depend on the temperature and are equal to 10.14 ± 0.08.

Table 5

pK_b values and parameters of equations (21) and (25)

T, K	pK_b(TZ)	**Equation** (21)				**Equation** (25)		
		$A_i \cdot 10^3$	$B_i \cdot 10^2$	C_i	R^2	A_i	B_i	R^2
273	6.89	0.578	8.24	0.541	0.9961	10.06	–235.1	0.9944
283	6.33	1.001	–0.214	1.972	0.9996	10.24	–277.5	0.9996
293	6.19	2.691	–15.58	5.101	0.9958	10.09	–295.8	0.9968
300	5.84	0.347	3.72	1.898	0.9992	10.10	–271.6	0.9979
308	6.06	2.686	–17.48	4.326	0.9936	10.14	–392.8	0.9835
313	5.19	-3.18	39.91	–3.068	0.9984	10.22	–276.7	0.9177

Conclusions

The influence of the amount of absorbed sulfur dioxide and temperature on the ion-molecular composition of "SO_2 – TZ – H_2O" solutions, their ionic strength, and electrochemical behavior has been determined. The composition of compounds formed during the chemisorption of SO_2 by an 0.1 mol/L aq.TZ solution has been identified. It was shown that formaldehyde addition to "SO_2 – $NH_2CH_2CH_2OH$ – H_2O" solutions leads to a decrease in the specific electrical conductivity of the system due to the formation of less mobile compounds. Further, a more detailed study of the mechanism of sulfur dioxide chemisorption by aqueous solutions of 1,3,5-triazines is planned. The obtained results are recommended for use in the development of effective sulfur dioxide chemisorbents.

References

[1] Grygorenko, O. O., Biitseva, A. V., Zhersh, S. (2018). Amino sulfonic acids, peptidosulfonamides and other related compounds. *Tetrahedron*, 74(13), 1355-1421. https://doi.org/10.1016/j.tet.2018.01.033

[2] Long, R. D., Hilliard, N. P., Chhatre, S. A. Timofeeva, T. V., Yakovenko, A. A., Dei, D. K., Mensah, E. A. (2010). Comparison of zwitterionic N-alkylaminomethanesulfonic acids to related compounds in the Good buffer series *Beilstein J. Org. Chem*. 6(31) https://doi.org/10.3762/bjoc.6.31

[3] Hrydina, T.L., Khoma, R. E., Ennan, A. A.-A., Fedchuk, A.S., Hruzevskyi, O. A. (2019). [Investigations of the antimicrobial activity of aminomethanesulfonic acids against strains of *Staphylococcus aureus* with different antimicrobial susceptibility]. *Zaporozhye Med. J*., 21(2), 234-239. https://doi.org/10.14739/2310-1210.2019.2.161502 (in Ukrainian).

[4] Khoma, R. E. (2019). [*Acid-base interaction and sulfooxidation at chemosorption alkylamines aqueous solutions*]. (Doctoral dissertation) http://ionc.com.ua/PDF/Khoma_thesis.pdf (in Ukrainian).

[5] Khoma, R.E., Baumer, V.N., Antonenko, P.B., Snihach, A.O., Godovan, V.V., Ennan, A.A., Dlubovskii, R.M., Gelmboldt, V. V. (2019). Synthesis, crystal structure, and spectral characteristics of N-(n-propyl)aminomethanesulfonic acid. Acute toxicity of aminomethanesulfonic acid and its N-alkylated derivatives. *Voprosy Khimii i Khimicheskoi Tekhnologii*., (6), 255. https://doi.org/10.32434/0321-4095-2019-127-6-255-262

[6] Khoma, R. E., Ennan, A. A.-A., Chebotaryov, A. N., Vodzinskii, S. V. (2019). [Aminomethansulfonic and alkylaminomethansulfonic buffer systems]. *Ukr. Chem. J.*, 85(9), 3–16. https://doi.org/10.33609/0041-6045.85.9.2019.3-16 (in Russian)

[7] Khoma, R. E., Ennan, A. A-A., Chebotaryov, A. N., Vodzinskii, S. V., Dlubovskii, R. M., Toporov, S. V. (2020). Electrochemical properties of aqueous solutions of sodium aminomethanesulfonates. *Ukr. Chem. J.*, 86(11), 51–64. https://doi.org/10.33609/2708-129X.86.11.2020.51-64

[8] Khoma, R., Ennan A. A.-A., Bienkovska, T. S., Osadchiy, L. T., Roy, E. L. (2021). Buffer systems based on aminometanesulphonate and monoethanolammonium N-alkylaminomethanes-ulphonates. *Visn. Odes. nac. univ. Him.*, *26*(2), 22–31. https://doi.org/10.18524/2304-0947.2021.2(78).233816

[9] Zhao L., Zhou Y., Yao Q., Wang Y., Ge S., Liu X. (2021). Calcium Scale Inhibition of Stimulated Oilfield Produced Water Using Polyaspartic Acid/Aminomethanesulfonic Acid. *ChemistrySelect*. *6*(15), 3692–3701. https://doi.org/10.1002/slct.202100853

[10] Zhang M., Peng C., Zhu M., Yan W., Jiang H., Nan G., Li M., Zhou Z. (2024). Multifunctional Zwitterionic Modification of SnO_2 in n–i–p Perovskite Solar Cells with Enhanced Fill Factor. *ACS Sustainable Chem. Eng.*, *12*(9). https://doi.org/10.1021/acssuschemeng.3c08004

[11] Kondratenko, Y. A. (2024). From alkanolamines to protic alkanolammonium ionic liquids. *J. Mol. Liq.*, *409*, 125460. https://doi.org/10.1016/j.molliq.2024.125460

[12] Deng T., Lv L., Li X., Wen J., Li H., Peng H., Chen H., Liu C., Bao L., Dang C., You Y., Chi F. (2025). Aminomethanesulfonic acid grafted polyamidoxime fibers with hydrophilicity, salt-tolerance and antimicrobial properties for highly efficient uranium extraction from seawater. *Sep. Purif. Technol.*, 356A, 129610. https://doi.org/10.1016/j.seppur.2024.129610

[13] Guo, A., Zhang, P., Ma, Y., Yuan, S. (2025). Molecular dynamics simulation of the electrochemical impact of aminomethanesulfonic acid on VO_2^+ in vanadium flow batteries. *Mater. Today Chem.* 47, 102815. https://doi.org/10.1016/j.mtchem.2025.102815

[14] Zuwaid, H. A. B. (2025). High-Yield Cellulose Hydrolysis Using Silica-Amino Methanesulfonic Acid Catalyst: Hidrolisis Selulosa Hasil Tinggi Menggunakan Katalis Asam Metanesulfonat Silika-Amino. *Academia Open. 10*(1). https://doi.org/10.21070/acopen.10.2025.10869

[15] Baker, M.V., Brown, D.H., Skelton, B.W., White, A.H. (1999). Chromium complexes of hydroxyl-functionalised 1,3,5-triazacyclohexanes. *J. Chem. Soc., Dalton Trans*. (9), 1483–1490. http://dx.doi.org/10.1039/a900122k

[16] Akhmadali, K., Guzal, K., Ravshan, A., Muzaffar, A. (2019). Influence of the structure of aldehydes on the directions of their reactions with monoethanolamine. *Chem. Chem. Eng.*, *2019*(2), 5. https://doi.org/10.70189/1992-9498.1110

[17] Fink, J. (2011). *Petroleum Engineer's Guide to Oil Field Chemicals and Fluids*. Saint Louis: Elsevier Science & Technology. https://doi.org/10.1016/C2009-0-61871-7

[18] Kapoor, R., Selvaraju, S. B., Subramanian, V., Yadav, J. S. (2024). Microbial Community Establishment, Succession, and Temporal Dynamics in an Industrial Semi-Synthetic Metalworking Fluid Operation: A 50-Week Real-Time Tracking. *Microorganisms*, 12(2), 267. https://doi.org/10.3390/microorganisms12020267

[19] Wylde, J., Taylor, G. (2019). Mercaptan scavenging revisited. *Clariant Oil Services.* https://www.clariant.com/-/media/Files/Business-Units/OMS/Oil-Services/Clariant-Article-in-Hydrocarbon-Engineering-2021-07-EN.pdf

[20] Romero, I., Kucheryavskiy, S., Maschietti, M. (2021). Experimental study of the aqueous phase reaction of hydrogen sulfide with MEA-triazine using in situ Raman spectroscopy. *Ind. Eng. Chem. Res.*, *60*, 15549–15557. https://doi.org/10.1021/acs.iecr.1c03833

[21] Romero I., Montero, F., Kucheryavskiy, S., Wimmer, R., Andreasen, A., Maschietti, M. (2023). Temperature- and pH-dependent kinetics of the aqueous phase hydrogen sulfide scavenging reactions with MEA-triazine. *Ind. Eng. Chem. Res.*, 62, 8569-8580. https://doi.org/10.1021/acs.iecr.3c00668

[22] Román M. N., Díaz M. A., Coll D. S. (2023). Study of the Reaction Mechanism of Triazines and Associated Species for H_2S Scavenging. *ACS Omega*, *8*(13), 12165–12172. https://doi.org/10.1021/acsomega.2c08103

[23] Romero I., Montero F., Kucheryavskiy S., Wimmer R., Andreasen A., Maschietti M. (2023). Temperature- and pH-Dependent Kinetics of the Aqueous Phase Hydrogen Sulfide Scavenging Reactions with MEA-Triazine. *Ind. Eng. Chem. Res.*, *62*(21), 8269–8280. https://doi.org/10.1021/acs.iecr.3c00668

[24] Tong, S., Zhu, J., Wang, Z., Yan, J. (2024). Highly Selective SO_2 Capture by Triazine-Functionalized Triphenylamine-Based Nanoporous Organic Polymers. *ACS Appl. Mater. Interfaces*, *16*(32), 42717–42725. https://doi.org/10.1021/acsami.4c08905

[25] Pourebrahimi, S., Pirooz, M., Kazemeini, M., Vafajoo, L. (2024). Synthesis, characterization, and gas (SO_2, CO_2, NO_2, CH_4, CO, NO, and N_2) adsorption properties of the CTF-1 covalent triazine framework-based porous polymer: experimental and DFT studies. *J. Porous Mater*. *31*, 643–657. https://doi.org/10.1007/s10934-023-01538-9

[26] Khoma, R. E. (2005) [*Acid-base interaction of sulfur dioxide with amides aqueous solutions*] (Unpublished habil. candidate's dissertation). A.V. Bogatsky Physico-Chemical Institute, Odesa, Ukraine (in Ukrainian).

[27] Khoma, R. E., Tsyganenko, K. V., Bienkovska, T. S., Ishkov, Yu. V., Vodzinskii, S. V. (2025). Sulfur dioxide interaction with monoethanolammonium and polyethylenepolyammonium citrates aqueous solutions products composition and the relative stability. *Ukr. Chem. J.*, 91(3), 3–24. https://doi.org/10.33609/2708-129X.91.3.2025.3-2

[28] Wang, J., Huang, W., Xu, H., Cui, P., Qu, Z., Yan, N. (2023). High-efficient cyclic absorption of sulfur dioxide in Na-Mg-Ci^{3-} compound system for wet flue gas desulfurization. *Sep. Purif. Technol*., *320*, 124138. https://doi.org/10.1016/j.seppur.2023.124138

[29] Vautherin, R., Métivier, H., Reguer, A., Benbelkacem, H. (2025). Use of a numerical model to evaluate SO_2 absorption efficiency by sodium sulfite in packed and spray columns. *Water Sci. Technol. 91*(8), 907–922. https://doi.org/10.2166/wst.2025.049